PHYSICAL REVIEW D **94,** 104008 (2016)

Quasinormal modes of nonlinear electromagnetic black holes from unstable null geodesics

Nora Bretón[1,†] and L. A. López[2,*]

[1]*Departamento de Física, Centro de Investigación y de Estudios Avanzados del I.P.N., Apdo. 14-740, Mexico D.F., Mexico*

[2]*Área Académica de Matemáticas y Física, UAEH, Carretera Pachuca-Tulancingo Km. 4.5, C. P. 42184, Pachuca, Mexico*

(Received 12 July 2016; published 3 November 2016)

The expressions for the quasinormal modes (QNM) of black holes with nonlinear electrodynamics, calculated in the eikonal approximation, are presented. In the eikonal limit QNM of black holes are determined by the parameters of the circular null geodesics. The unstable circular null orbits are derived from the effective metric that is the one obeyed by light rays under the influence of a nonlinear electromagnetic field. As an illustration we calculate the QNM of four nonlinear electromagnetic black holes, two singular and two regular, namely, from Euler-Heisenberg and Born-Infeld theories, for singular ones, and the magnetic Bardeen black hole and the one derived by Bronnikov for regular ones. Comparing with the QNM of the linear electromagnetic counterpart, their Reissner-Nordström black hole is done.

DOI: 10.1103/PhysRevD.94.104008

I. INTRODUCTION

When a black hole (BH) undergoes perturbations, the resulting behavior can be described in three stages. The first stage corresponds to radiation due to the initial conditions of the perturbations. The second stage corresponds to damped oscillations with complex frequencies. The modes of such oscillations are called quasinormal modes (QNM). The frequencies of QNM are independent of initial perturbations, since they are the intrinsic imprint of the response of the black hole to external perturbations. The third stage in general corresponds to a power law decay of the fields.

Besides the importance of QNM in the analysis of black hole stability, they play an outmost role in characterizing gravitational wave signals, as the ones recently detected at LIGO, as well as the promised ones jointly with VIRGO collaboration and the planned space antenna project LISA [1]. QNM resonances, being the characteristic "sound" of the BH itself, are crucial to identify the spacetime parameters, especially the mass and angular momentum of the BH, but are also important in identifying additional physical parameters arising from more realistic BH models. In fact precise observations of the late-time ringdown signal show the differences in the QNM spectrum [2] and they can be used to rule out bizarre BHs. QNM from BHs is a thoroughly studied subject; for recent reviews [3–6] can be consulted and references therein.

There are also theoretical reasons that justify the study of QNM, one of them from loop quantum gravity. It has been observed that for asymptotically flat BHs, the real part of the high overtones of QNM coincides with the Barbero-Immirzi parameter [7]; this parameter measures the size of the quantum area in Planck units in relation to the counting of microstates in the mentioned theory.

Since early studies on Schwarzschild BH perturbations [8] gravitational waves coming from the "vibrations of a BH" were identified as gravitational waves in spiral orbits close to the unstable circular orbits, the BH being not a source but a temporal storage of high-frequency gravitational radiation [9]. Mashhoon and Ferrari [10,11] have suggested an analytical technique of calculating the QNM in the geometric-optics (eikonal) limit. The basic idea is to interpret the BH free oscillations in terms of null particles trapped at the unstable circular orbit and slowly leaking out. The real part of the QNM frequencies is determined by the angular velocity at the unstable null geodesic; the imaginary part is related to the instability time scale of the orbit in such a way that QNM can be determined from the unstable null geodesics that are the orbits attached to the maximum of the effective potential barrier felt by light rays on their interaction with the BH. In this sense Cardoso [12] showed the relationship among unstable null geodesics, Lyapunov exponents, and quasinormal modes in a stationary spherically symmetric spacetime.

It is well known that in situations involving strong electromagnetic fields, the linear superposition does not hold and nonlinear effects, for instance the creation of electron-positron pairs or scattering of light by light, are very likely to occur. These situations are described by quantum electrodynamics; alternatively, classical theories that include these nonlinear phenomena in an effective way may be useful. Among these theories are the Euler-Heisenberg (EH) [13] and Born-Infeld (BI) [14] theories. Moreover, nonlinear electromagnetic theories have attracted attention lately due to their ability to suppress the singularity in some BH solutions. As a result of the

*lalopez@uaeh.edu.mx
†nora@fis.cinvestav.mx

nonlinear interaction, light rays do not follow the null geodesics of the background metric, but do follow the null geodesics of an effective metric that depends on the nonlinear electromagnetic energy momentum tensor [15–18]. Extensive research has been done on nonlinear electromagnetism in curved backgrounds; see for instance [19] and references therein.

In [20] applying the ideas of Cardoso, the QNM frequencies of the regular magnetic BH model proposed by Bardeen were determined; Bardeen BH is a solution of nonlinear electrodynamics coupled to Einstein gravity. QNM of nonlinear electromagnetic BHs were computed, using the WKB method, for the Born-Infeld BH in [21] and for the Bronnikov BH in [22]. Our study differs from previous ones in the fact that we use the effective metric to determine the unstable circular orbits followed by light rays. Otherwise the frequencies of the QNM correspond to massless test particles that indeed follow, in the eikonal approximation, the null geodesics of the background metric. Those QNM frequencies do not correspond to light rays that in the presence of strong electromagnetic fields do interact among themselves, giving rise to nonlinear effects.

Using the effective metric and the corresponding effective potential, we derive the Lyapunov exponent expression that is related to the imaginary part of the QNM frequencies; as an illustration we address two examples of singular BHs: the Born-Infeld BH and a magnetic Euler-Heisenberg one, as well as two examples of regular BHs, the Bardeen model for a magnetic self-gravitating BH, and one solution derived by Bronnikov. Quasinormal modes of regular black holes have been analyzed in [23].

The paper is organized as follows: In Sec. II we give a brief explanation for determining the QNM frequencies using the unstable null geodesics and the Lyapunov exponent. In Sec. III a short summary of the nonlinear electrodynamics for a static spherically symmetric spacetime is presented as well as the effective nonlinear electromagnetic metric. In Sec. IV the expressions for the real and imaginary parts of the QNM frequencies in terms of the nonlinear Lagrangian are given. In Sec. V we analyze the QNM frequencies of the four examples mentioned above. In each case the QNM frequencies are compared with the ones corresponding to the massless test particles and light rays of the Reissner-Nordstrom (RN) BH that is the linear counterpart of nonlinear electromagnetic BHs. Conclusions are given in the last section.

II. QNM AND THE LYAPUNOV EXPONENT

The connection between the QNM and bound states of the inverted BH effective potential was pointed out in [11]. In [12] it was shown that, in the eikonal limit, the QNM of BHs in any dimensions are determined by the parameters of the circular null geodesics. The real part of the complex QNM frequencies is determined by the angular velocity at the unstable null geodesics. The imaginary part is related to the instability time scale of the orbit, and therefore related to the Lyapunov exponent that is its inverse. Lyapunov exponents are a measurement of the average rate at which nearby trajectories converge or diverge in the phase space. A positive Lyapunov exponent indicates a divergence between nearby trajectories, i.e., a high sensitivity to initial conditions. In the case of stationary, spherically symmetric spacetimes it turns out that this exponent can be expressed as the second derivative of the effective potential evaluated at the radius of the unstable circular null orbit. The agreement of the so calculated QNM with the analytic WKB approximation,

$$\omega_{\mathrm{QNM}} = \Omega_c l - i\left(n+\frac{1}{2}\right)|\lambda|, \tag{1}$$

where n is the overtone number and l is the angular momentum of the perturbation, was also shown. Ω_c is the angular velocity at the unstable null geodesic and λ is the Lyapunov exponent, determining the instability time scale of the orbit. From the equations of motion for a test particle in the static spherically symmetric (SSS) spacetime, $\dot{r}^2 = V_r$, where V_r is the effective potential for radial motion, circular geodesics are determined from the conditions $V(r_c) = V'(r_c) = 0$, and r_c is the radius of the circular orbit. The Lyapunov exponent in terms of the second derivative of the effective potential is given by

$$\lambda = \sqrt{\frac{V_r''}{2\dot{t}^2}}, \tag{2}$$

where t is the time coordinate. The dot denotes the derivative with respect to an affine parameter and the prime stands for the derivative with respect to r. The orbital angular velocity is given by

$$\Omega_c = \frac{d\varphi}{dt} = \frac{\dot{\varphi}}{\dot{t}}. \tag{3}$$

For our purposes both expressions should be evaluated at r_c, the radius of the unstable null circular orbit. Its impact parameter b_c is related to the effective potential by $V_r = 1/{b_c}^2$, i.e., the energy at infinity of those orbits is equal to the maximum of the effective potential.

For a static spherically symmetric background

$$ds^2 = f(r)dt^2 - \frac{1}{g(r)}dr^2 - r^2 d\Omega^2, \tag{4}$$

the energy E and the angular momentum L of a test particle are conserved quantities,

$$f(r)\dot{t} = E = \text{const}, \qquad r^2\dot{\varphi} = L = \text{const}. \tag{5}$$

For equatorial orbits ($\theta = \pi/2$), the equation for radial motion is $\dot{r}^2 = V_r$. For the case of a static spacetime $f = g$ in (4), the effective potential is given by

$$V_r = g(r)\left[\frac{E^2}{f(r)} - \frac{L^2}{r^2}\right] = E^2 - f\frac{L^2}{r^2}. \tag{6}$$

Then the Lyapunov exponent, related to the imaginary part of the QNM frequencies, from (2) is given by

$$\lambda^2 = \frac{f_c}{2r_c^2}[2f_c - r_c^2 f_c''], \tag{7}$$

while the orbital angular velocity, which is proportional to the real part of the QNM frequencies, is given by

$$\Omega_c = \frac{L}{r_c^2}\frac{f_c}{E} = \sqrt{\frac{f_c}{r_c^2}}. \tag{8}$$

In the previous expressions (7) and (8) the conditions for a circular orbit, $V_r = 0$ and $V_r' = 0$, that amount, respectively, to

$$\frac{E^2}{L^2} = \frac{f}{r^2}, \quad \text{and} \quad 2f - rf' = 0, \tag{9}$$

have been incorporated.

In the following section Eqs. (7) and (8) are determined from the effective metric, and λ and Ω_c are written in terms of the nonlinear electromagnetic (NLEM) Lagrangian.

III. QNM OF NLEM BHS FROM THE EFFECTIVE METRIC

The action for gravitation coupled to an electromagnetic field is given by

$$S = \frac{1}{16\pi}\int d^4x\sqrt{-g}[R - L(F)], \tag{10}$$

where R is the scalar curvature and L is an arbitrary function of the electromagnetic invariant $F = F^{\mu\nu}F_{\mu\nu}$, with $F_{\mu\nu} = \partial_\mu A_\nu - \partial_\nu A_\mu$ being the electromagnetic field tensor. For the Maxwell theory the Lagrangian is directly proportional to F, $L_M = F$. We note that the most general Lagrangian can depend on both electromagnetic invariants, F and $G = \mathcal{F}^{\mu\nu}F_{\mu\nu}$, where $\mathcal{F}^{\mu\nu}$ is the dual field-strength electromagnetic tensor. These kinds of generalizations are also connected to Gauss-Bonnet corrections [24]. In this work we restrict ourselves to Lagrangians depending only on F but that are otherwise completely general. Roughly speaking this restriction has the consequence of having solutions with only electric or magnetic charges, but not both.

The electromagnetic tensor compatible with spherical symmetry has two nonzero components, $F_{01} = -F_{10}$ and $F_{23} = -F_{32}$, corresponding to the radial electric and magnetic fields, with

$$r^2 L_F F^{10} = q_e, \qquad F_{23} = q_m \sin\theta, \tag{11}$$

where q_e and q_m are the electric and magnetic charges, respectively, while the subindex F means the derivative with respect to F. Adopting the definitions

$$\begin{aligned} f_e &= 2F_{01}F^{10} = 2q_e^2 L_F^{-2} r^{-4} \geq 0, \\ f_m &= 2F_{23}F^{23} = 2q_m^2 r^{-4} \geq 0, \end{aligned} \tag{12}$$

$F = f_m - f_e$ and the energy-momentum tensor can be written as

$$\begin{aligned} T^\mu_\nu = \frac{1}{2}\mathrm{diag}(&L + 2f_e L_F, L + 2f_e L_F, L \\ &- 2f_m L_F, L - 2f_m L_F). \end{aligned} \tag{13}$$

The nonlinearity of the electromagnetic field modifies light trajectories that regularly are the null geodesics of the background metric $g_{\mu\nu}$. In nonlinear electromagnetism, instead, photons do propagate along null geodesics of an effective geometry with the metric tensor $\gamma^{\mu\nu}_{\text{eff}}$ that depends on the nonlinear theory. The discontinuities of the electromagnetic field propagate by obeying the equation for the characteristic surfaces. Then the effective metric can be derived from the analysis of the characteristic surfaces [15,16,25]. The corresponding equation for the gradient of the characteristic surfaces $S_{,\mu}$ is

$$(L_F g^{\mu\nu} - 4L_{FF}F^\mu_\alpha F^{\alpha\nu})S_{,\mu}S_{,\nu} = \gamma^{\mu\nu}_{\text{eff}} S_{,\mu}S_{,\nu} = 0. \tag{14}$$

Calculating the metric components $\gamma^{\mu\nu}_{\text{eff}}$, the effective metric of the SSS spacetime is given by

$$\begin{aligned} ds^2_{\text{eff}} = &(L_F G_m)^{-1} \\ &\times\left\{G_m G_e^{-1}\left(f(r)dt^2 - \frac{1}{f(r)}dr^2\right) - r^2 d\Omega^2\right\}. \end{aligned} \tag{15}$$

G_m and G_e, the magnetic and electric factors that make the difference between the linear and nonlinear electromagnetism, are given by

$$G_m = \left(1 + 4L_{FF}\frac{q_m^2}{L_F r^4}\right), \qquad G_e = \left(1 - 4L_{FF}\frac{q_e^2}{L_F^3 r^4}\right), \tag{16}$$

and in the linear limit become equal to 1. In determining null geodesics conformal factors can be ignored, since they do not modify the null geodesics. Considering the geodesic

motion in the equatorial plane of the effective spacetime (15), not including the conformal factor $(L_F G_m)^{-1}$, the corresponding effective potential V_r is

$$V_r = G_m^{-1} G_e \left[G_m^{-1} G_e E^2 - \frac{f(r) L^2}{r^2} \right]. \tag{17}$$

When we apply the first conditions for the (unstable) null circular orbits $V(r_c) = 0$, we obtain

$$\frac{E^2}{L^2} = \left(\frac{G_m}{G_e} \right)_{r_c} \frac{f_c}{r_c^2}, \tag{18}$$

and jointly with the second condition, $V'(r_c) = 0$, the radius r_c of the circular null orbit is given by one of the roots of the following equation:

$$\left(\frac{G_e}{G_m} \right) \left(\frac{f_c'}{f_c} - \frac{2}{r_c} \right) - \left(\frac{G_e}{G_m} \right)'_{r_c} = 0. \tag{19}$$

Such a root should be greater than the horizon radius, $r_c > r_h$; subscript "c" means that the quantity in question is evaluated at the radius $r = r_c$. This radius is also known as the radius of the photosphere, and defines the sphere of unstable circular photon trajectories. For the Schwarzschild BH $r_c = 3M$.

The Lyapunov exponent (2) for the effective metric takes the form

$$\lambda^2 = \frac{f_c r_c^2}{2} \left[\frac{f_c}{r_c^2} \frac{G_m}{G_e} \left(\frac{G_e}{G_m} \right)''_c - \left(\frac{f}{r^2} \right)''_c \right], \tag{20}$$

while the angular velocity (3) changes to

$$\Omega_c = \sqrt{\frac{G_m}{G_e} \frac{f_c}{r_c^2}}. \tag{21}$$

Equations (20) and (21), the nonlinear electromagnetic version of Eqs. (7) and (8), determine the QNM frequencies, imaginary and real parts, respectively, for NLEM BHs in the eikonal approximation.

From the expressions (16) and having determined the sign of L_{FF}/L_F it can be defined whether G_m and G_e are greater or less than 1. From that knowledge and the expression of Ω_c we can assert whether the real part of the QNM frequencies is enhanced or suppressed as compared to the linear counterpart. For instance if $L_{FF}/L_F < 0$ then $G_m \leq 1$ and $G_e > 1$ and consequently, from (21), Ω_c gets a smaller value, resulting in a suppression of the real part of the QNM frequencies ω_r.

The analysis is not so straightforward for the imaginary part, Eq. (20), since it is not obvious what the sign of the second derivative of G_e/G_m will be. In this case we need more specific information about the NLEM Lagrangian.

In the next section examples of different NLEM BHs are given and the QNM frequencies due to the NLEM field are compared with those corresponding to massless test particles as well as with the QNM frequencies originated from the SSS solution to the Einstein-Maxwell equations, the Reissner-Nordström BH.

IV. EXAMPLES

We calculate the QNM frequencies of four SSS BH solutions corresponding to different NLEM theories coupled to gravity. The first two examples of singular NLEM BHs, the Born-Infeld and a magnetic solution for the Euler-Heisenberg electrodynamics coupled to gravity, are addressed. Then we analyze the QNM response of two regular NLEM BHs: the Bardeen magnetic monopole and one Bronnikov solution. A comparison with massless particles and linear electromagnetism is established as well. Only the fundamental frequency $n = 0$ is considered, that is, the least damped mode.

A. The QNM of the Reissner-Nordström black hole

The RN black hole is the SSS solution to the action (10) with $L = F$, $L_F = 1$, and $L_{FF} = 0$ and then the nonlinear factors are $G_e = 1$ and $G_m = 1$. In what follows, the QNM behavior of each addressed example is compared with that corresponding to the RN BH. Now the RN case is briefly exposed.

In the eikonal or geometric-optics limit, the QNM frequencies are given by (1) with λ and Ω_c calculated as in (7) and (8), respectively. For the RN BH, the metric function in the line element (4) is given by

$$f(r) = g(r) = 1 - \frac{2M}{r} + \frac{Q^2}{r^2}, \tag{22}$$

while the circular null orbit radius r_c is calculated from (9), which in the RN case amounts to the quadratic polynomial

$$r_c^2 - 3M r_c + 2Q^2 = 0, \qquad r_c = \frac{3}{2}\left(1 + \sqrt{1 - 8Q^2/9}\right), \tag{23}$$

where we have used a dimensionless coordinate $r \to r/M$ and $Q \to Q/M$. The functions λ and Ω_c are given by (7) and (8),

$$\lambda^2 = \frac{1}{r_c^6}(r_c^2 - 2Q^2)(Q^2 + r_c^2 - 2r_c),$$
$$\Omega_c^2 = \frac{1}{r_c^4}(r_c^2 - 2r_c + Q^2), \tag{24}$$

which substituting r_c from (23) gives

TABLE I. Comparison of the QNM of test particles characterized by $s = 1$, $l = 1$, and $n = 0$ interacting with the Schwarzschild BH, calculated using different methods. The eikonal approximation underestimates the real frequencies and overestimates the imaginary ones.

Schwarzschild QNM	
Numerical	$0.2483 - 0.092i$
Third order WKB	$0.2459 - 0.0931i$
Sixth order WKB	$0.2482 - 0.092i$
Eikonal limit	$0.19245 - 0.096225i$

$$\lambda^2 = \frac{4\sqrt{1-8Q^2/9}(1+3\sqrt{1-8Q^2/9})}{3^3(1+\sqrt{1-8Q^2/9})^4},$$
$$\Omega_c^2 = \frac{2(1+3\sqrt{1-8Q^2/9})}{27(1+\sqrt{1-8Q^2/9})^3}. \tag{25}$$

These are the expressions (also derived in [26]) that we use in the comparisons with the NLEM cases. In the RN case analytic solutions can be found all the way through. Analytic solutions were not determined in any of the following examples. Recent works on aspects of RN QNM are [27–29].

Table I gives an idea about how accurate the eikonal approximation is compared with other methods; the Schwarzschild case is illustrated. The eikonal numbers are obtained from Eqs. (25) with $Q = 0$. A thorough discussion on the comparison between the accuracy of different methods of calculating the QNM can be consulted in [6].

B. Born-Infeld black hole

The BI nonlinear electrodynamics was first considered by Born and Infeld in an attempt to cure at the classical level the singularity of the electric field of a point charge [14]. Born-Infeld electrodynamics possesses several interesting physical features like the absence of birefringence, the Maxwell limit for the weak electromagnetic field, as well as the finiteness of the electric field at the charge position. The Einstein-Born-Infeld (EBI) generalization of the RN BH was obtained by García *et al.* in [30]; the geodesic structure of the EBI BH was studied in [31] and recently in [32]. This Einstein-Born-Infeld solution is singular at the origin and it is characterized by three parameters: mass, charge, and the BI parameter b that is the maximum attainable electromagnetic field; the EBI BH can present one, two, or zero horizons depending on the values of the parameters. The Born proposed Lagrangian is given by

$$(L(F) = 4b^2\left(-1+\sqrt{1+\frac{F}{2b^2}}\right). \tag{26}$$

Exact BH solutions are known; see for instance Sec. VIII in [33]. In [34] the stability and QNM of these BHs has been analyzed in the context of the tensor-vector-scalar theory. Here, we address the so-called BI solution that for a line element of the form (4) is given by the metric function

$$f(r) = g(r) = 1 - \frac{2M}{r} + \frac{2}{3}r^2b^2\left(1-\sqrt{1+\frac{q^2}{b^2r^4}}\right) + \frac{2}{3}\frac{q^2}{r}\sqrt{\frac{b}{q}}\mathbb{F}\left(\arccos\left[\frac{br^2/q-1}{br^2/q+1}\right],\frac{1}{\sqrt{2}}\right), \tag{27}$$

where $\mathbb{F}$ is the elliptic integral of the first kind, M is the mass parameter, q is the electric charge (both in length units), and b is the Born-Infeld parameter that corresponds to the magnitude of the electric field at $r = 0$. The nonvanishing component of the electromagnetic field is $F_{rt} = q(r^4 + \frac{q^2}{b^2})^{-1/2}$. The nonlinear factors G_m and G_e, in the case in which only electric charge is considered, $q_m = 0$, are

$$G_m = 1, \qquad G_e = \left(1+\frac{q^2}{b^2r_c^4}\right). \tag{28}$$

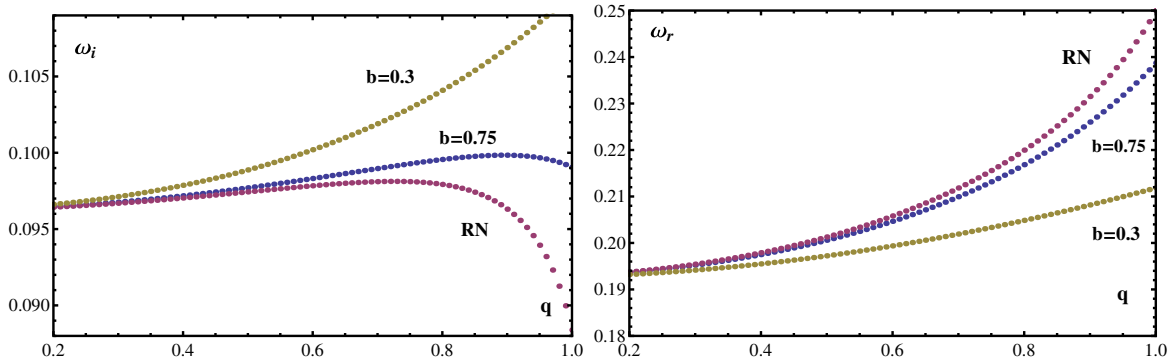

FIG. 1. The behavior of ω_i and ω_r for the BI and RN BHs is shown as a function of the charge. Two values of b were considered, $b = 0.3$ and $b = 0.75$; the other parameters are fixed: $M = 1$ and $n = 0$.

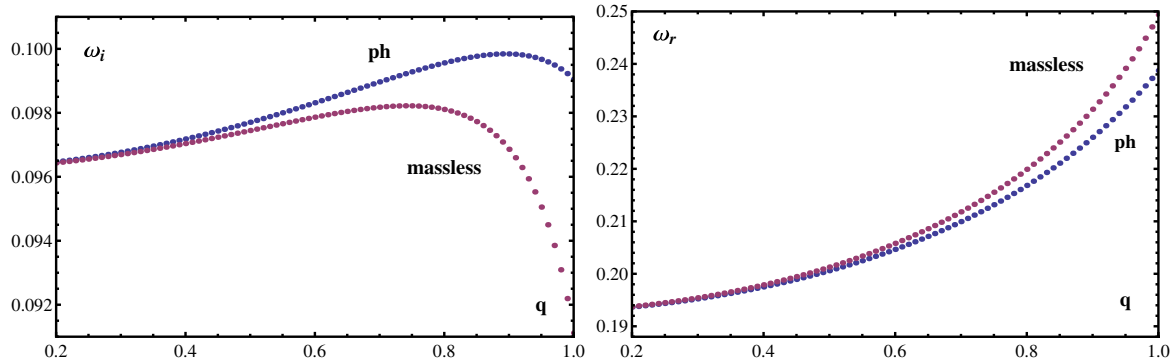

FIG. 2. Comparison between ω_i and ω_r of the BI BH for massless particles and photon (ph) frequencies is shown. The rest of the parameters are $M = 1$, $b = 0.75$, and $n = 0$. As $q \to 0$ both BHs approach the Schwarzschild case.

Hereafter we consider $\omega_r/l \mapsto \omega_r$ for our analysis. In Fig. 1 the behavior of the QNM frequencies ω_i and ω_r of the BI BH for two different values of the parameter b is shown; those are then compared with RN BHs. The imaginary part of QNM frequencies ω_i, for the RN case, increases as q augments and presents a maximum then decreases; for the RN BH the value of q cannot exceed $q = 1$, which corresponds to the extreme BH, $q = M$. The BI BH does not have this constraint, and ω_i increases without bound for small values of b. Therefore BI-ω_i is enhanced as compared with the RN BH. The opposite occurs with the real part of the QNM frequencies, BI-ω_r, that is suppressed as compared with the RN BH. Both frequencies approach the RN limit as b increases.

The QNM frequencies coming from massless particles and photons (ph) are compared in Fig. 2. For the imaginary part, ω_i, the previous behavior is enhanced even more for photon trajectories, while ω_r-massless particle values are greater than the photon's. Massless test particle QNM frequencies were analyzed in [21] using the WKB approximation up to sixth order. Our results definitively agree qualitatively, and the same tendency is observed: imaginary frequencies are enhanced as the BI parameter decreases while the real ones are suppressed in the same limit.

TABLE II. Behavior of the QNM frequencies for the BI BH as calculated for massless particles using a sixth order WKB method and for photons using the eikonal approximation. The parameters are fixed as $n = 0$, $l = 2$, $b = 0.4$, and $M = 1$.

BI BH	WKB method		Effective metric	
q	ω_r	ω_i	ω_r	ω_i
0.2	0.481698	0.068375	0.386888	0.0965409
0.4	0.498791	0.069957	0.393042	0.097527
0.6	0.530753	0.072592	0.40396	0.0993303
0.7	0.554740	0.074309	0.411548	0.100636
0.8	0.586874	0.076306	0.420782	0.102317
0.9	0.631678	0.078624	0.43188	0.104523
1	0.699423	0.081372	0.445116	0.107521

Quantitatively there is no agreement, first because we are in the eikonal approximation, and second because the discrepancy is precisely the nonlinear effect that is not present for massless particles (gravitational perturbations). In Table II the QNM frequencies calculated in the eikonal limit are compared with the ones for massless test particles obtained using a sixth order WKB in [21]. As the charge grows the difference narrows for the imaginary frequencies while the opposite occurs for the real frequencies. Table II illustrates the discrepancy in QNM between the electromagnetic and gravitational perturbations, which is shown in Fig. 2 as well.

C. Euler-Heisenberg black hole

The effective action for electrodynamics due to one-loop quantum corrections was calculated by EH. For the low-frequency limit $\omega \ll m_e c^2/h^2$ the effective Lagrangian with magnetic charge [35] takes the form

$$L(F) = F(1 - aF), \tag{29}$$

with $a = he^2/(360\pi^2 m_e^2)$, where h, e, and m_e are the Planck constant, electron charge, and electron mass, respectively. BI theory applies for fields even stronger than the ones in QED, because it turns out that a Lagrangian very similar to (29) can be obtained in the weak field limit of the BI Lagrangian: expanding the square root in (26) up to second order, $(1+x)^{1/2} = 1 + x/2 - x^2/8 + \cdots$, we obtain

$$L(F) = 4b^2\left(-1 + 1 + \frac{F}{4b^2} + \frac{F^2}{32b^4} + \cdots\right) = F - \frac{F^2}{8b^2}. \tag{30}$$

From the comparison with (29) a relationship between the EH and BI parameters is obtained, $8b^2 = a^{-1}$. For the previous reasons we expect a very similar behavior for the EH-QNM frequencies and the BI-QNM frequencies. This is the case indeed.

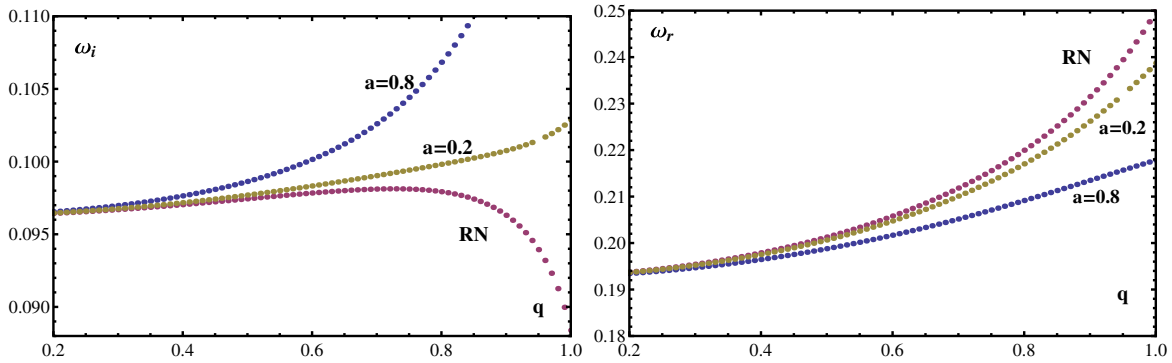

FIG. 3. The behavior of ω_i and ω_r in terms of the charge q is shown for the EH and RN BHs; the rest of the parameters are fixed as $M = 1$ and $n = 0$

In [35] a solution of the EH field coupled to gravity equations was found (see also [36]). It corresponds to a SSS magnetic BH with metric elements in (4) given by

$$f(r) = g(r) = 1 - \frac{2M}{r} + \frac{q^2}{r^2} - \frac{2}{5}a\frac{q^4}{r^6}, \qquad (31)$$

where M is the mass parameter and q is the magnetic charge. One or two horizons may occur: if $(M/q)^2 \leq 24/25$ a single horizon exists but for $(M/q)^2 > 24/25$ a second and a third horizon occurs. Extremal solutions exist only for $a^2 \leq a^2_{\rm crit} = (8/27)q^2$. The electromagnetic invariant is $F = 2q^2/r^4$. Since $q_e = 0$, the G_e and G_m factors are

$$G_e = 1, \qquad G_m = \left(1 + \frac{8aq^2}{4aq^2 - r_c^4}\right). \qquad (32)$$

The behavior of QNM frequencies ω_i and ω_r for the EH BH resembles the BI ones (see Fig. 3), taking into account that the nonlinear parameters b and a are inversely proportional. For small a's we obtain an effect similar to large b's, i.e., the behavior approaches the RN one when $a \mapsto 0$,

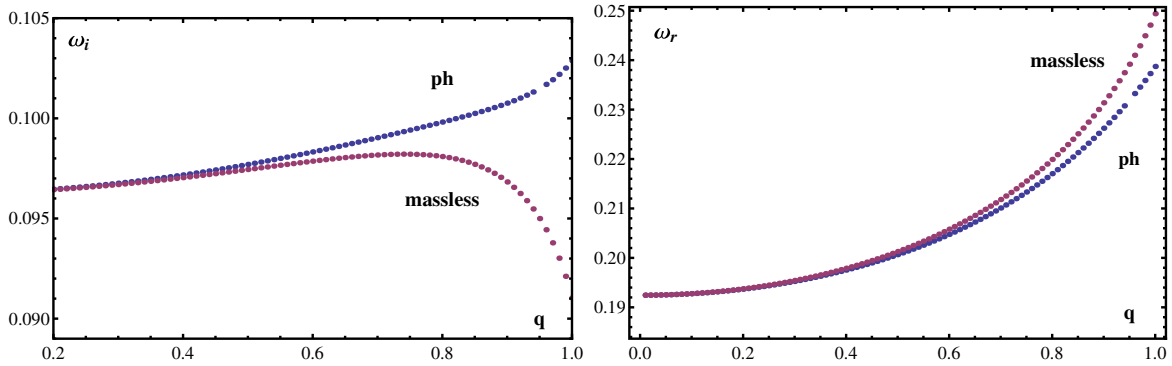

FIG. 4. Comparison of photon vs massless particle QNM frequencies is shown, with imaginary and real parts, ω_i and ω_r, of the EH BH varying the magnetic charge. In this plot $M = 1$, $a = 0.2$, and $n = 0$

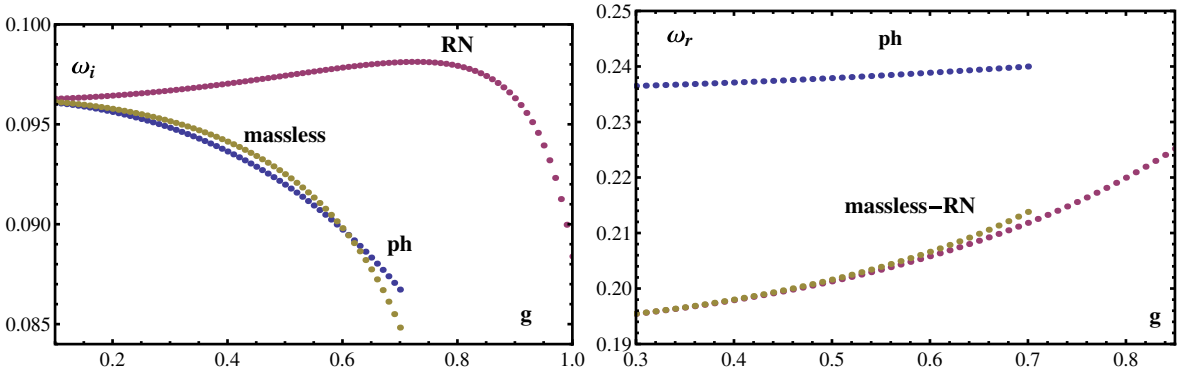

FIG. 5. The behavior of ω_i and ω_r of the Bardeen BH as functions of the charge g, keeping fixed $M = 1$ and $n = 0$.

TABLE III. Comparison of the QNM frequencies from test fields with $n = 0$, $l = 2$, and $M = 1$ using a sixth order WKB for the bardeen BH [20] and the effective metric for photons in the eikonal approximation. As the charge grows the differences are enhanced for both real and imaginary frequencies,

Bardeen BH	WKB method		Effective metric	
g	ω_r	ω_i	ω_r	ω_i
0.1	0.484470	0.0966541	0.47158	0.0960758
0.2	0.48699	0.0963019	0.47304	0.0956186
0.3	0.491380	0.0956563	0.472984	0.0948243
0.4	0.497895	0.0946064	0.47422	0.0936395
0.5	0.507037	0.0929337	0.475814	0.091981
0.6	0.519668	0.0901727	0.477752	0.091981
0.7	0.537388	0.0851340	0.479982	0.0867285

while for larger a's the departure from RN behavior is clear, enhanced for ω_i and suppressed for ω_r. Regarding the massless-photon comparison, ω_i is enhanced and ω_r is suppressed for photons with respect to massless particle trajectories as can be seen in Fig. 4. As far as we know a QNM study of this BH has not been presented previously.

D. Bardeen black holes

This model was proposed by Bardeen in the 1960s as an example of a regular BH; later on Ayón-Beato and García [37] found a nonlinear electromagnetic source for such a BH. Accordingly, the Bardeen BH can be interpreted as a self-gravitating nonlinear magnetic monopole with mass M and magnetic charge $q_m = g$, derived from Einstein gravity coupled to the nonlinear Lagrangian

$$L(F) = \frac{6}{sg^2}\frac{(g^2F/2)^{\frac{5}{4}}}{(1+\sqrt{g^2F/2})^{\frac{5}{2}}}, \tag{33}$$

where $s = |g|/2M$. It has been shown that this Lagrangian does not have the correct weak field limit [38], [26]. The solution for the coupled Einstein and NLEM Lagrangian (33) for a static spherically symmetric space is given by

$$f(r) = g(r) = 1 - \frac{2Mr^2}{(r^2+g^2)^{\frac{3}{2}}}. \tag{34}$$

In [39] is presented a study on the scattering and absorption cross section as well as the quasinormal modes of the Bardeen BH. In [40] the geodesic motion is addressed. The solution (34) presents horizons only if $2s = g/m \leq 0.7698$. The electromagnetic invariant is $F = 2g^2/r^4$ and the G_e and G_m factors are given by

$$G_e = 1, \qquad G_m = 1 - \frac{4(6g^2 - r^2)}{8(r^2+g^2)}. \tag{35}$$

Note that for $g \mapsto 0$ the correct limit $G_m = 1$ is not achieved; instead $G_m(g \mapsto 0) = 3/2$. The radius of the unstable circular orbit r_c is found numerically from (19) with (34) and (35) and care must be taken so that such a root is greater than the horizon radius, $r_c > r_h$.

The behavior of the QNM from light rays impinging upon the Bardeen BH is shown in Fig. 5. ω_i decreases when g increases for both massless particles and photons. This behavior is in contrast with the two previously analyzed examples; the resemblance with RN ω_i occurs only when the charge approaches zero. Regarding ω_r the behavior for massless particles is indistinguishable from the RN one. The one corresponding to photons is odd in the sense that even in the limit that charge goes to zero the RN behavior is not recovered; one possible explanation may be the nature of the solution because charge and mass parameters are not independent, and in fact when charge turns off, so does the mass whose origin is purely electromagnetic. Moreover, as it was pointed out before, the Lagrangian (33) does not have the appropriate weak field limit. QNM frequencies for massless particles have been determined in [20]; in a similar fashion as for the BI BH, our results are in good qualitative agreement; as for the quantitative agreement some discrepancies exist, attributable to nonlinear electromagnetic effects felt by photons and not by massless test particles. Table III shows some comparative values to get insight into the discrepancy between the respective frequencies.

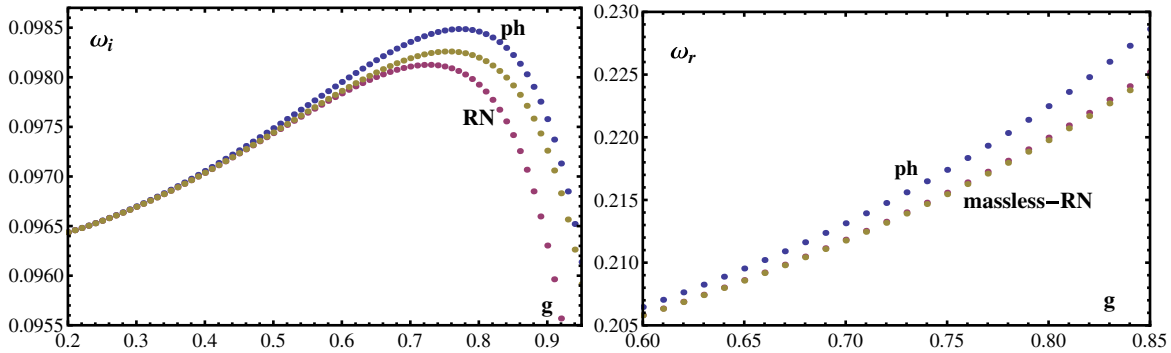

FIG. 6. QNM frequencies ω_i and ω_r of the Bronnikov BH are shown as functions of the charge g; the other parameters are fixed to $M = 1$ and $n = 0$.

TABLE IV. The QNM frequencies for the Bronnikov magnetic BH with $n = 0$, $l = 2$, and $M = 1$ comparing the eikonal limit with a WKB approximation given in [22].

Bronnikov BH	WKB method		Effective metric	
g	ω_r	ω_i	ω_r	ω_i
0.1	0.458758	0.0951121	0.385544	0.0962784
0.2	0.461174	0.0952761	0.387518	0.0964377
0.3	0.465284	0.0955432	0.390938	0.0966995
0.4	0.471218	0.095901	0.39603	0.0970555
0.5	0.479186	0.096326	0.403162	0.0974872

E. Bronnikov magnetic black hole

In [38] NLEM Lagrangians coupled to gravity were analyzed focusing on the properties that lead to nontrivial regular metrics. No-go theorems forbid regular electric BHs, but magnetic ones can be found. One example is presented in the same reference, with the Lagrangian

$$L(F) = F\mathrm{sech}^2[a(F/2)^{1/4}], \tag{36}$$

where a is a constant. The metric function in the line element of the form (4) is

$$f(r) = g(r) = 1 - \frac{g^{3/2}}{ar}\left[1 - \tanh\left(\frac{a\sqrt{g}}{r}\right)\right], \tag{37}$$

where the constant a is related to the mass m and the magnetic charge g by $a = g^{3/2}/(2M)$. The solution corresponds to a BH if $M/g > 0.96$. The electromagnetic invariant is $F = 2g^2/r^4$. For a purely magnetic charge $G_e = 1$ and

$$G_m = \frac{g^2\sinh^2(\frac{g^2}{2Mr})(-2g^2 + g^2\cosh(\frac{g^2}{2Mr}) - 5Mr\sinh(\frac{g^2}{2Mr}))}{4Mr(-4Mr^3 + g^2\tanh(\frac{g^2}{2Mr}))}. \tag{38}$$

The QNM frequency behavior when the charge is varying is shown in Fig. 6. The imaginary part of the QNM frequencies ω_i for massless particles as well as for photons reproduces the RN behavior, and slight departure is observed only when the charge approaches its upper limit. As for the real part of the QNM frequencies, ω_r, for massless particles it is coincident with RN for any charge, while a small difference occurs for photons. From all of the examined examples the Bronnikov BH is the one in which the nonlinear effects are the least.

Table IV compares the QNM frequencies calculated for the effective metric in the eikonal approximation with the ones obtained in [22] with WKB. Definitively there is a qualitative agreement, and the same tendency is observed. The discrepancies diminish in the imaginary frequencies when the charge increases while the opposite happens for the real parts.

V. CONCLUSIONS

We have studied the QNM frequencies of NLEM BHs through the Lyapunov exponent in the optical approximation. QNM frequencies were calculated from the unstable null geodesics of the effective metric. The effective metric is obtained from the background metric but taking into account the NLEM effects. From the expressions of the real and imaginary parts of the QNM frequencies and Eqs. (20) and (21), it is clear that the NLEM effects modify QNM frequencies, enhancing or suppressing them depending on the sign of the quotients L_{FF}/L_F and of the second derivative of G_e/G_m. The NLEM effects manifest on the dynamics of the light perturbations modifying the oscillation periods as well as the damping times.

The obtained QNM frequencies, in the eikonal approximation, are calculated to four SSS BH solutions corresponding to different NLEM theories coupled to gravity. In all cases comparison is done with the QNM frequencies of the linear counterpart, the RN back hole. In three of the examples (the BI, EH, and Bronnikov solution), the NLEM effect when the charge is varied consists in suppressing the real part while increasing the imaginary one, i.e., oscillation periods are larger and relaxation occurs faster.

Comment apart deserves the Bardeen BH. In this case the effect is the opposite: the real part of the QNM frequencies is enhanced while the imaginary part is suppressed; notoriously the real frequency is not recovered when the charge approaches zero. Several explanations come to mind; among them is that mass and charge parameters are not independent in this solution and the limit to zero of the charge cannot be taken separately from the value of the mass, since the origin of the mass is magnetic; this is a self-gravitating magnetic structure. Additionally, the comparison between the behavior of massless particles and photons was done.

A thorough analysis is needed to know how the modifications introduced by NLEM effects influence the BH stability; steps in this direction are given in [26]. Another point of interest would be checking if there is any consequence to introducing NLEM related to the conjectured relationship between the real part of the QNM frequencies and the BH area quantization.

ACKNOWLEDGMENTS

N. B. acknowledges partial support of CONACyT (Mexico), Grant No. 166581.

[1] B. P. Abbott *et al.*, Observation of Gravitational Waves from a Binary Black Hole Merger, Phys. Rev. Lett. **116**, 061102 (2016).
[2] V. Cardoso, E. Franzin, and P. Pani, Is the Gravitational-Wave Ringdown a Probe of the Event Horizon?, Phys. Rev. Lett. **116**, 171101 (2016); Erratum, Phys. Rev. Lett. **117**, 089902(E) (2016).
[3] H.-P. Nollert, Quasinormal modes: the characteristic "sound" of black holes and neutron stars, Classical Quantum Gravity **16**, R159 (1999).
[4] K. D. Kokkotas and B. G. Schmidt, Quasinormal modes of stars and black holes, Living Rev. Relativ. **2**, 2 (1999).
[5] R. A. Konoplya and A. Zhidenko, Quasinormal modes of black holes: from astrophysics to string theory, Rev. Mod. Phys. **83**, 793 (2011).
[6] E. Berti, V. Cardoso, and A. O. Starinets, Quasinormal modes of black holes and black branes, Classical Quantum Gravity **26**, 163001 (2009).
[7] G. Kunstatter, d-Dimensional Black Hole Entropy Spectrum from Quasinormal Modes, Phys. Rev. Lett. **90**, 161301 (2003).
[8] W. H. Press, Long wave trains of gravitational waves from a vibrating black hole, Astrophys. J. **170**, L105 (1971).
[9] C. J. Goebel, Comments on the"vibration" of a black hole, Astrophys. J. **172**, L95 (1972).
[10] B. Mashhoon, Stability of charged rotating black holes in the eikonal approximation, Phys. Rev. D **31**, 290 (1985).
[11] V. Ferrari and B. Mashhoon, New approach to the quasinormal modes of a black hole, Phys. Rev. D **30**, 295 (1984).
[12] V. Cardoso, A. S. Miranda, E. Berti, H. Witek, and V. T. Zanchin, Geodesic stability, Lyapunov exponents, and quasinormal modes, Phys. Rev. D **79**, 064016 (2009).
[13] J. S. Schwinger, On gauge invariance and vacuum polarization, Phys. Rev. **82**, 664 (1951).
[14] M. Born and L. Infeld, Foundations of the new field theory, Proc. R. Soc. A **144**, 425 (1934).
[15] S. A. Gutierrez, A. L. Dudley, and J. F. Plebanski, Signals and discontinuities in general relativistic nonlinear electrodynamics, J. Math. Phys. (N.Y.) **22**, 2835 (1981).
[16] M. Novello, V. A. De Lorenci, J. M. Salim, and R. Klippert, Geometrical aspects of light propagation in nonlinear electrodynamics, Phys. Rev. D **61**, 045001 (2000).
[17] Y. N. Obukhov and G. F. Rubilar, Fresnel analysis of the wave propagation in nonlinear electrodynamics, Phys. Rev. D **66**, 024042 (2002).
[18] F. Abalos, F. Carrasco, R. Goulart, and O. Reula, Nonlinear electrodynamics as a symmetric hyperbolic system, Phys. Rev. D **92**, 084024 (2015).
[19] G. W. Gibbons and K. Hashimoto, Nonlinear electrodynamics in curved backgrounds, J. High Energy Phys. 09 (2000) 013.
[20] S. Fernando and J. Correa, Quasinormal modes of Bardeen black hole: scalar perturbations, Phys. Rev. D **86**, 064039 (2012).
[21] S. Fernando, Gravitational perturbation and quasinormal modes of charged black holes in Einstein-Born-Infeld gravity, Gen. Relativ. Gravit. **37**, 585 (2005).
[22] J. Li, K. Lin, and N. Yang, Nonlinear electromagnetic quasinormal modes and Hawking radiation of a regular black hole with magnetic charge, Eur. Phys. J. C **75**, 131 (2015).
[23] A. Flachi and J. P. S. Lemos, Quasinormal modes of regular black holes, Phys. Rev. D **87**, 024034 (2013).
[24] S. H. Hendi, Einstein-Maxwell gravity with additional corrections, Eur. Phys. J. C **73**, 2634 (2013).
[25] E. G. de Oliveira Costa and S. E. P. Bergliaffa, A classification of the effective metric in nonlinear electrodynamics, Classical Quantum Gravity **26**, 135015 (2009).
[26] E. Chaverra, J. C. Degollado, C. Moreno, and O. Sarbach, Black holes in nonlinear electrodynamics: quasinormal spectra and parity splitting, Phys. Rev. D **93**, 123013 (2016).
[27] M. Richartz and D. Giugno, Quasinormal modes of charged fields around a Reissner-Nordström black hole, Phys. Rev. D **90**, 124011 (2014).
[28] C. Corda, S. H. Hendi, R. Katebi, and N. O. Schmidt, Hawking radiation—quasinormal modes correspondence and effective states for nonextremal Reissner-Nordström black holes, Adv. High Energy Phys. **2014**, 527874 (2014).
[29] S. H. Hendi, Asymptotic Reissner-Nordström black holes, Ann. Phys. (Amsterdam) **333**, 282 (2013).
[30] A. D. García, H. I. Salazar, and J. F. Plebański, Type-D solutions of the Einstein and Born-Infeld nonlinear-electrodynamics equations, Nuovo Cimento Soc. Ital. Fis. **84B**, 65 (1984).
[31] N. Breton, Geodesic structure of the Born-Infeld black hole, Classical Quantum Gravity **19**, 601 (2002).
[32] R. Linares, M. Maceda, and D. Martinez-Carbajal, Test particle motion in the Born-Infeld black hole, Phys. Rev. D **92**, 024052 (2015).
[33] G. W. Gibbons and D. A. Rasheed, Electric-magnetic duality rotations in nonlinear electrodynamics, Nucl. Phys. **B454**, 185 (1995).
[34] P. D. Lasky and D. D. Doneva, Stability and quasinormal modes of black holes in tensor-vector-scalar theory: scalar field perturbations, Phys. Rev. D **82**, 124068 (2010).
[35] H. Yajima and T. Tamaki, Black hole solutions in Euler-Heisenberg theory, Phys. Rev. D **63**, 064007 (2001).
[36] V. A. De Lorenci, N. Figueiredo, H. H. Fliche, and M. Novello, Dyadosphere bending of light, Astron. Astrophys. **369**, 690 (2001).
[37] E. Ayon-Beato and A. Garcia, The Bardeen model as a nonlinear magnetic monopole, Phys. Lett. B **493**, 149 (2000).
[38] K. A. Bronnikov, Regular magnetic black holes and monopoles from nonlinear electrodynamics, Phys. Rev. D **63**, 044005 (2001).
[39] C. F. B. Macedo, E. S. de Oliveira, and L. C. B. Crispino, Scattering by regular black holes: planar massless scalar waves impinging upon a Bardeen black hole, Phys. Rev. D **92**, 024012 (2015).
[40] Z. Stuchlk and J. Schee, Circular geodesic of Bardeen and Ayon-Beato-Garcia regular black-hole and no-horizon spacetimes, Int. J. Mod. Phys. D **24**, 1550020 (2015).